



DISCLAIMER

This report has been prepared by the Institute of Geological and Nuclear Sciences Limited (GNS Science) exclusively for and under contract to EQC Research Foundation. Unless otherwise agreed in writing by GNS Science, GNS Science accepts no responsibility for any use of or reliance on any contents of this report by any person other than EQC Research Foundation and shall not be liable to any person other than EQC Research Foundation, on any ground, for any loss, damage or expense arising from such use or reliance.

Use of Data:

Date that GNS Science can use associated data: 1 January 2015

BIBLIOGRAPHIC REFERENCE

Rhoades, D.A.; Mueller, C.; Buxton, R.; Gerstenberger, M.C. 2015. Ionospheric Earthquake Precursors, *GNS Science Consultancy Report 2015/06*. 26 p.

CONTENTS

EXECUTIVE SUMMARY.....	III
NON-TECHNICAL SUMMARY	IV
1.0 INTRODUCTION	1
2.0 COMPUTATION OF TIME-VARYING TEC FIELD FROM GPS DATA.....	3
2.1 OPEN SOURCE SOFTWARE TOOLKIT.....	3
2.2 COMPUTATIONAL PROCEDURE	3
3.0 VARIATION OF TEC OBSERVATIONS BEFORE SELECTED LARGE EARTHQUAKES	7
3.1 SELECTED EARTHQUAKES	7
3.2 MAXIMUM AND MEAN TEC VERSUS TIME	7
3.3 DEGREE OF ANOMALY SCALE.....	12
3.4 SPATIAL DISTRIBUTION OF TEC ANOMALIES	13
3.5 COMPARISON WITH ANOMALIES OBSERVED IN PREVIOUS STUDIES.....	16
4.0 INDEX OF LOCAL TEC ANOMALY	18
4.1 DEFINITION OF INDEX.....	18
4.2 PLOTS OF LOCAL CORRELATION INDEX.....	20
5.0 CONCLUSION.....	24
6.0 ACKNOWLEDGEMENTS.....	25
7.0 REFERENCES	25

FIGURES

Figure 1	Location of grid points at which TEC is estimated for each time of observation.....	6
Figure 2	Lower: Maximum of TEC (y-axis) over the New Zealand region versus time in the period 2010/08/17 to 2010/09/10.....	8
Figure 3	Lower: Maximum of TEC (y-axis) over the New Zealand region versus time in the period 2011/02/05 to 2011/03/03.....	8
Figure 4	Lower: Maximum of TEC (y-axis) over the New Zealand region versus time in the period 2013/07/04 to 2013/07/23.....	9
Figure 5	Lower: Maximum of TEC (y-axis) over the New Zealand region versus time in the period 2013/07/30 to 2013/08/26.....	9
Figure 6	Lower: Mean of TEC (y-axis) over the New Zealand region versus time in the period 2010/08/17 to 2010/09/10.....	10
Figure 7	Lower: Mean of TEC (y-axis) over the New Zealand region versus time in the period 2011/02/05 to 2011/03/03.....	10
Figure 8	Lower: Mean of TEC (y-axis) over the New Zealand region versus time in the period 2013/07/04 to 2013/07/23.....	11
Figure 9	Lower: Maximum of TEC (y-axis) over the New Zealand region versus time in the period 2013/07/30 to 2013/08/26.....	11

Figure 10	Spatial distribution of TEC over the New Zealand region at the time of the highest anomaly of maximum TEC preceding the Darfield earthquake.	13
Figure 11	Spatial distribution of TEC over the New Zealand region at the time of the highest anomaly of mean TEC preceding the Darfield earthquake.	14
Figure 12	Spatial distribution of TEC over the New Zealand region at the time of the highest anomaly of maximum and mean TEC preceding the Christchurch earthquake.....	15
Figure 13	Spatial distribution of TEC over the New Zealand region at the time of the highest anomaly of mean TEC preceding the Lake Grassmere earthquake.....	16
Figure 14	Plot of local correlation index versus time for the nearest grid point to each major earthquake (a) Darfield, (b) Christchurch, (c) Seddon, and (d) Lake Grassmere.	21
Figure 15	Spatial variation of local correlation index on 18 February 2011, the time of greatest anomaly in the index prior to the Christchurch earthquake.....	22

TABLES

Table 1	Selected major earthquakes and associated time periods for TEC analysis.	7
Table 2	Lead time and degree of anomaly of highest value of maximum and mean TEC in the lead up to each major earthquake.	12

EXECUTIVE SUMMARY

Anecdotal studies suggest that ionospheric disturbances sometimes occur as short-term precursors to earthquakes with a precursor time of several days. This study initiates an examination of possible ionospheric earthquake precursors in New Zealand, with a view to systematically testing their value for short-term earthquake forecasting.

GPSTk software produced by the University of Texas at Austin to compute Total Electron Content (TEC) in the ionosphere from GPS network observations has been adapted to the New Zealand region. It has been used to estimate the TEC in the ionosphere on a spatial grid of locations surrounding the New Zealand region for selected periods preceding and following four recent major earthquakes – the M 7.1 2010 Darfield earthquake, M6.3 2011 Christchurch earthquake, M 6.5 2013 Seddon earthquake and M 6.6 2013 Lake Grassmere earthquake. The software gives snapshots of the spatial variation of TEC over New Zealand at 30 second intervals.

The time series of maximum and mean regional TEC, in the lead-up to the four earthquakes, was studied in a search for precursory anomalies. TEC has strong daily fluctuations, with high values during daytime and near-zero values at night-time. Significant higher-than-normal TEC anomalies were found for the Darfield, Christchurch and Lake Grassmere earthquakes with precursor times ranging from 7–11 days. Despite the similarities of the precursor times, the spatial distributions of TEC at the times of these anomalies suggest that they are unrelated to the earthquake concerned and more likely due to solar or geomagnetic effects. They are different from proposed ionospheric precursors in the literature, in which the anomalies are seen as local variations to the pattern of TEC variation close to the location of forthcoming earthquakes.

A local correlation index was defined to identify TEC anomalies which are more likely to be related to earthquake occurrence. This is a daily index that compares the variation of TEC within a day at each point of the grid with the average daily variation at nearby surrounding grid points. It is designed to distinguish local variations in TEC from the large scale variations caused by solar and geomagnetic influences. Most values of the index are very close to one. A value much less than one is anomalous.

The local correlation index was plotted for the same time periods before and after the four selected earthquakes, for the grid point closest to each earthquake source. For the Christchurch earthquake, the index showed an anomalously low value with a precursor time of three days. For the other earthquakes no precursor anomaly was observed.

A short-term precursor can be quite informative for earthquake forecasting, even if it occurs only for some of the major earthquakes. It is proposed that future studies should extend the database of TEC observations to a much longer period. Then the local correlation could be used as a systematic input for the formation of hybrid short-term earthquake forecasting models. In that way its information value for earthquake forecasting, over and above what is already known about how the likelihood of earthquake occurrence varies in time and space, could be determined.

NON-TECHNICAL SUMMARY

Disturbances in the total electron content (TEC) of the ionosphere have been reported as proposed short-term precursors to earthquakes in some regions, with a lead time of several days. In this project we computed TEC in the New Zealand region, with a view towards testing the value of TEC anomalies for short term earthquake forecasting. We adapted software produced by the University of Texas to compute TEC from GPS network observations. We mapped TEC in the ionosphere on a spatial grid covering the whole of New Zealand, at half-minute intervals, for several weeks before, and a few days after, four recent major earthquakes – the 2010 Darfield, 2011 Christchurch, 2013 Seddon and 2013 Lake Grassmere earthquakes.

TEC has strong daily fluctuations, with high values during daytime and near-zero values at night-time. Also, TEC averaged over the whole region was found to have anomalously high spikes preceding three of the four earthquakes, with lead times ranging from 7–11 days. However, the spatial distributions of TEC at the times of these spikes suggest that they are probably due to solar or geomagnetic effects and not related to earthquake occurrence. They are different from anomalies in the literature, which show local perturbations of the daily fluctuations of TEC close to the location of forthcoming earthquakes.

A local correlation index was defined for each point in the spatial grid, to find TEC anomalies that are more likely to be related to earthquakes. Most values of the index are very close to one. A value much less than one is anomalous. The index showed an anomalously low value near to the location of the Christchurch earthquake three days before its occurrence. The lead time of three days is typical for proposed ionospheric earthquake precursors. The index showed no local anomaly in the lead up to the Darfield, Seddon and Lake Grassmere earthquakes.

A short-term precursor can be quite informative for earthquake forecasting, even if it occurs only for some of the major earthquakes. Future studies should extend the database of TEC observations to a much longer period. The local correlation index should then be used as one possible systematic input to short-term earthquake forecasting models. Its information value can best be measured in combination with other inputs, which include what we already know about how the likelihood of earthquake occurrence varies in time and space.

1.0 INTRODUCTION

Anecdotal studies suggest the possible existence of a relation between Total Electron Content (TEC) in the ionosphere and earthquake occurrence, with a lag time of about three days between the ionospheric disturbance and the occurrence of a major earthquake. Our aim is to assess the potential for TEC to contribute to short-term earthquake forecasting in New Zealand, and to prepare a database derived from TEC measurements that could be used as input to future regional earthquake likelihood models in the New Zealand Earthquake Forecast Testing Centre.

Retrospective analyses have identified ionospheric anomalies preceding some well-known earthquakes, including the 1999 M7.7 Chi-Chi and other earthquakes in Taiwan (Liu et al., 2000, 2001, 2002), the 2003 M6.6 San Simeon earthquake in California (Pulinets et al., 2004), the 1995 M7.2 Kobe earthquake in Japan (Hayakawa, 2007), the 2006 Kithara earthquake in Greece (Zakharenkova et al., 2007), the 2004 M>9 Sumatra and other earthquakes in Indonesia (Saroso et al., 2008), and the 2008 M7.9 Wenchuan earthquake in China (Zhou et al., 2009). We are not aware of any previous studies of ionospheric precursors in relation to New Zealand earthquakes.

TEC can be derived from dual frequency GPS observations. The existence in New Zealand of a substantial network of continuous GPS stations gives us the opportunity to track changes in TEC with time and location over the New Zealand region with reasonable spatial resolution, and hence to attempt to systematically relate such changes to earthquake occurrence. Derived TEC measurements could add considerable value, at relatively low cost, to the existing GeoNet database of GPS observations.

The objectives of this study are:

1. Calculate TEC from New Zealand continuous GPS stations data, back-dating the calculations as far as possible.
2. Conduct a preliminary data analysis of variation in the temporal and spatial correlation in the TEC series prior to selected New Zealand earthquakes.
3. Compare the patterns revealed by the data analysis with those reported in similar studies of other regions.
4. Develop an index that reflects the strength of a localised TEC anomaly at a given location and time. Such an index could be used as input to modify the earthquake occurrence rate density in a regional earthquake likelihood model.

The first step, i.e., the generation of a database of TEC observations, is the major part of this study, because it requires implementing the necessary software systems from scratch.

A key step in (2) and (4) is to discriminate ionospheric signals caused by solar and geomagnetic disturbances from those caused by the preparation processes of earthquakes (Pulinets and Liu, 2004; Afraimovich and Astafaya, 2008). The majority of ionospheric signals are caused by solar or geomagnetic disturbances, and are therefore well correlated spatially over wide regions. A minority of ionospheric signals are thought to originate from the ground. Signals from the ground have only a local effect. Therefore, when a strong signal originates from the ground, the signal in the region of the ionosphere above it should become de-correlated from the signal in neighbouring regions. Such de-correlation is the anomaly to look for as a potential earthquake precursor.

The study of ionospheric earthquake precursors (Liu et al., 2001, 2002) is a growing area of research activity. It is a major branch of the burgeoning field of seismo-electromagnetics (Uyeda et al., 2009). The whole field is somewhat controversial because of the anecdotal nature of much of the research to date.

The TEC is one way of measuring ionospheric disturbance. It is derived from the propagation delay experienced by GPS signals in the ionosphere, which is an important error source affecting GPS positioning. It is calculated from the differential delay between signals on two different carrier frequencies along the ray path between the ground receiver and the satellite, with corrections applied for the changing ray path length as the satellite elevation angle varies (Manucci et al., 1993; Calais and Minster, 1995; Liu et al., 2004; Surotkin et al., 2007; Dautermann et al., 2007).

Physical explanations of coupling between seismicity and ionospheric disturbance have been offered by Pulinets (2004). A variety of physical explanations have been given for ground electromagnetic emissions, including stress changes in rocks through piezoelectric and piezomagnetic effects (Bishop, 1981), induction effects due to motion of electric charges in the geomagnetic field (Revel et al., 1999), the emission of radioactive gas or metallic ions, or positive-hole defects in minerals (Freund, 2000). Models proposed to link electromagnetic effects at ground level with ionospheric signals include direct coupling from the Earth's surface to the lower ionosphere through electric currents (Pulinets et al., 2000; Sorokin et al., 2001) and the triggering of atmospheric gravity waves by gas releases or thermal anomalies (Molchanov and Hayakawa, 2001; Pulinets, 2007).

Previous studies have tended to concentrate on finding anomalous ionospheric signals before a few individual large earthquakes. This is a focus of the present study also, but it is not the desired endpoint of our research programme into ionospheric precursors. Anecdotal examples of ionospheric anomalies preceding large earthquakes are now sufficiently numerous that additional anecdotes, positive or negative, can hardly affect the current status of the science. Therefore (1) and (4) are seen as the most important objectives in this study. The importance of objectives (2) and (3) is to give guidance on how the index in (4) should be constructed.

The viability of empirical analyses of coupling between seismicity and TEC anomalies is strongly affected by the spatial extent and length of time-period covered by the available TEC series and the number of significant earthquakes in the region over the relevant time period. The conclusions from a study based on only a few earthquakes are inevitably tentative, whatever the outcome. The statistical confidence in the results grows as the database of TEC measurements and earthquakes increases. This study initiates the setting up of a database of TEC measurements and derived statistics, which, as it is augmented in time, will eventually be capable of providing a clear result.

This study is therefore preparatory to future endeavours to make TEC in the ionosphere, estimated from signals received at continuous New Zealand GPS stations, an authorised database for models submitted to the New Zealand earthquake forecast testing centre. The index developed in (4) could then be used to develop and test one or more short-term earthquake forecasting models. By this means, the information value of ionospheric precursors can be rigorously and transparently assessed (Schorlemmer et al., 2007).

2.0 COMPUTATION OF TIME-VARYING TEC FIELD FROM GPS DATA

2.1 OPEN SOURCE SOFTWARE TOOLKIT

Total electron content has been computed using the GPSTk Open Source Toolkit for GPS Processing, Total Electron Content Effects, Measurements and Modelling (<http://www.gpstk.org>, Gaussiran et al., 2004). The availability of this open source toolkit, which is a product of the Space and Geophysics Laboratory within the Applied Research Laboratories of the University of Texas at Austin, made the successful execution of this project possible.

A considerable effort was first made to implement total electron content computations using an alternative computing tool, made available to this project through our late colleague John Beavan by Eric Calais. Dautermann, Calais et al. (2007) applied this method for a study in southern California. Considerable technical difficulties arose in attempting to adapt this software to New Zealand. A disadvantage of this method compared to the GPSTk toolkit is that it provides estimates of total electron content for a single ground-based receiver station by averaging over the satellites in its vicinity. In contrast, the GPSTk toolkit maps the TEC over a whole region by interpolating between the points where all the signals between ground-based receivers and satellites pass through the ionosphere. The latter approach is much more suitable for our purposes. Once the availability of the GSPTk software suite became known to us, the attempt to implement the method of Dautermann, Calais et al. (2007) was abandoned.

2.2 COMPUTATIONAL PROCEDURE

This section describes how TEC is computed in GPSTk. The passages below are extracted, with only minor modifications, from Gaussiran et al. (2004), where further details can also be found.

The GPSTk software was developed at the Applied Research Laboratories of The University of Texas at Austin for GPS research.

The GPSTk software suite includes an application that involves processing GPS data for remote sensing of the ionosphere. It takes data from a large set of receivers that are distributed within a compact geographical region and computes a contour map of the ionospheric vertical TEC. This analysis adopts the common model assumption that the ionosphere consists of a thin shell at a fixed height, usually 350 or 400 kilometres, surrounding Earth. The two-dimensional (latitude, longitude) density of free electrons in this shell is called the total electron content or TEC of the ionosphere. The TEC signal is measured in TEC units (TECU) where one TECU = 10^{16} electrons/m².

The GPS satellites broadcast a ranging signal to estimate the distance (or “range”) between the satellite and receivers on the ground. Because the transmit time and the receive time are different, it is impossible to measure the true range between the satellite and the receiver. The apparent distance that is estimated is called the pseudorange, because it includes unaccounted for receiver clock errors. The ranging signal is broadcast on dual frequency bands from an altitude of 20,200 km, substantially above the ionosphere. Thus the GPS

signals pass through the ionosphere, in general at an oblique angle. The electron content of the ionosphere disperses and delays the signals. The delay, and the TEC along the line of sight, or 'slant TEC', that produces it, is computed from the ranging signals as follows:

$$TEC_{slant} = \frac{(R_1 - R_2)}{\alpha} TECU_{perM} \quad (2.1)$$

where

$$\alpha = \frac{f_1}{f_2} - 1, \quad (2.2)$$

and

$$TECU_{perM} = \frac{f_1^2}{20.48} \times 10^{-16}. \quad (2.3)$$

Here pseudorange observations are denoted with symbol R and subscripts refer to GPS frequencies. $TECU_{perM}$ is a constant that converts metres to TECU. The constant α depends only on the two GPS broadcast frequencies f_1 and f_2 .

The slant TEC is related to the vertical TEC ($VTEC$) by an obliquity factor, computed from simple geometric considerations.

$$VTEC = TEC_{slant} \times obliquity \quad (2.4)$$

with

$$obliquity = \sqrt{1 - a^2} \quad (2.5)$$

$$a = \frac{R \cos(e)}{R + h}, \quad (2.6)$$

where e is the elevation of the satellite as seen from the receiver on the surface of the Earth, R is the radius of the Earth and h is the height of the ionosphere.

The point at which the signal crosses the model ionospheric shell is called the ionospheric pierce point or IPP. The IPP for a given satellite and receiver can be computed from the receiver position and the observed elevation and azimuth angles of the satellite as seen at the receiver, along with the height of the ionosphere. If the angle subtended at the centre of the Earth by the receiver and the IPP is

$$p = \frac{\pi}{2} - e - \sin^{-1}(a), \quad (2.7)$$

then the latitude ϕ_{IPP} and longitude λ_{IPP} of the IPP are:

$$\phi_{IPP} = \sin^{-1}(\sin(\phi) \cos(p) + \cos(\phi) \sin(p) \cos(a)) \quad (2.8)$$

$$\lambda_{IPP} = \lambda + \sin^{-1}(\sin(p) \sin(a) / \cos(\phi)), \quad (2.9)$$

where the receiver position is given by latitude and longitude (ϕ, λ) and (e, a) are the observed elevation and azimuth of the satellite. The radius of the IPP is the same as that of the ionosphere, $R+h$.

The GPS measurement of ionospheric TEC is complicated by delays that exist in both the satellite and the GPS receiver. These arise from differing path lengths for the two GPS signal frequencies; they are essentially constant over short periods (days), but vary over longer timescales. The sum of the two biases, *satellite + receiver*, may be estimated using GPS data, provided the ionospheric TEC is known or modelled.

The procedure to account for these delays is first to estimate the ‘satellite plus receiver’ biases from the night-time portion of the data, when the ionospheric TEC is negligibly small. Then the estimated biases are applied to the slant TEC measurements, from which the vertical TEC is computed. This data, along with the estimated biases, are then used to fit a simple model ionosphere at the points of a two dimensional grid at the ionospheric height using a weighted least squares estimator.

The first step is pre-processing of the raw data. The GPSTk uses an extended version of the Receiver Independent Exchange (RINEX) file format, which allows intermediate results, as well as the raw data, to be stored within the RINEX format. The GPSTk application “ResCor” uses dual frequency range data from the input RINEX file, obtained from GeoNet to compute the slant ionospheric delay, the latitude and longitude of the IPP, and the elevation and azimuth of the satellite. It stores the results in an ‘extended’ RINEX format file. The output file includes, in the file header, a unique label for the receiver as well as the receiver position.

A GPSTk program called “IonoBias” simultaneously reads all the pre-processed files, limiting consideration to data collected during the local night-time hours. IonoBias applies all the TEC data to a least squares fit of both a simple model of the (night-time) ionospheric TEC and all the biases:

$$VTEC = bias + obliquity \times F(\phi, \lambda), \quad (2.10)$$

where the function F represents the model of the ionosphere. In what follows, wherever the term “TEC” is used, it means “VTEC”.

The process of calculating TEC with the GPSTk software was adapted to the New Zealand GPS data and automated by Christof Mueller. The automation system is implemented as a module in the versatile python scripting language that runs GPSTk components in a batch like process. The system runs efficiently through the steps required to create TEC maps for any given time span. Currently it is feasible to generate TEC maps over the New Zealand region at 30 second intervals over a two week period. Calculation times are of the order of several tens of hours after optimization of the system through multi-threading (i.e., parallel processing). The set of 2880 maps generated for a single day provide a detailed description of the variation of estimated TEC over New Zealand during that day. At each time point the TEC is estimated at 450 locations on an approximately rectangular grid, as shown in Figure 1.

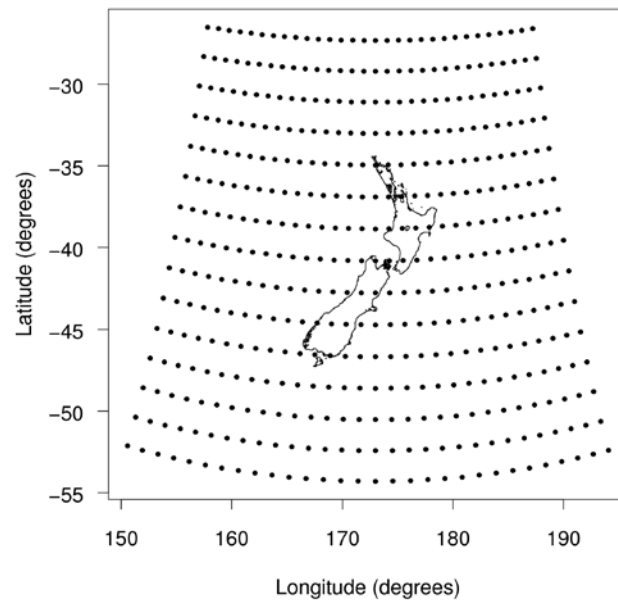


Figure 1 Location of grid points at which TEC is estimated for each time of observation.

3.0 VARIATION OF TEC OBSERVATIONS BEFORE SELECTED LARGE EARTHQUAKES

3.1 SELECTED EARTHQUAKES

The computing time to execute TEC map calculations is such that it was not feasible with the resources of this project to produce a continuous record at 30 second intervals for the whole period for which GPS data are available. Accordingly, attention has been restricted to the periods preceding four recent major earthquakes in New Zealand, as listed in Table 1.

Table 1 Selected major earthquakes and associated time periods for TEC analysis.

Earthquake name	Time of occurrence (UT)	Location (Lat., Long)	Depth (km)	Magnitude (M _L)	Period of TEC computations
Darfield	2010/09/03 16:35	-43.53, 172.17	11.0	7.1	2010/08/17–2010/09/13
Christchurch	2011/02/21 23:51	-43.58, 172.68	5.4	6.3	2011/02/05–2011/03/03
Seddon	2013/07/21 05:09	-41.60, 174.33	12.9	6.5	2013/07/04–2013/07/31
Lake Grassmere	2013/08/16 2:31	-41.73, 174.15	8.2	6.6	2013/07/30–2013/08/26

3.2 MAXIMUM AND MEAN TEC VERSUS TIME

Here we summarise the time variation of the spatial maximum of TEC over the New Zealand region for the period preceding each of these four major earthquakes, starting two weeks before (Figure 2–Figure 5). These plots show that there is a strong daily variation of TEC, with daily maxima around noon and low values close to zero during the night. This pattern is consistent with most of the TEC signal being of solar origin.

Figure 2–Figure 5 also show that in each case the highest value of the time series occurred between 7 and 11 days before the major earthquake. In the case of the Lake Grassmere earthquake (Figure 5), an equally high value occurred seven days after the earthquake. Visually, the highest value appears most anomalous in the case of the Christchurch earthquake (Figure 3) and least anomalous in the case of the Seddon earthquake (Figure 4).

Figure 6–Figure 9 show similar plots for the mean TEC over the New Zealand region. The TEC anomaly is now visually more distinct prior to the Darfield earthquake (c.f. Figure 6 and Figure 2), equally distinct prior to the Christchurch earthquake (c.f. Figure 7 and Figure 3), slightly less indistinct prior to the Seddon earthquake (c.f. Figure 8 and Figure 4), and more distinct prior to the Lake Grassmere earthquake (c.f. Figure 9 and Figure 5). In the latter case the anomaly seven days after the earthquake is no longer comparable to the one 11 days before it.

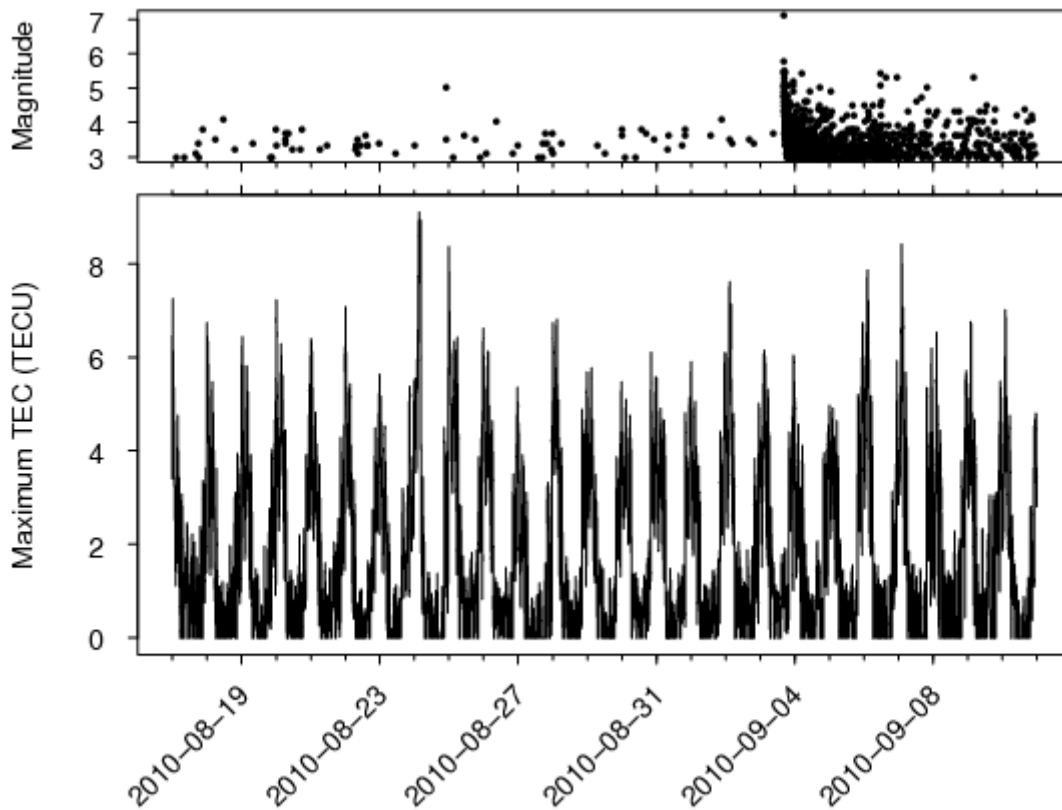


Figure 2 Lower: Maximum of TEC (y-axis) over the New Zealand region versus time in the period 2010/08/17 to 2010/09/10. Upper: Magnitude versus time of occurrence for earthquakes in the New Zealand region with magnitude $M \geq 3.0$, including the Darfield earthquake of 2010/09/03.

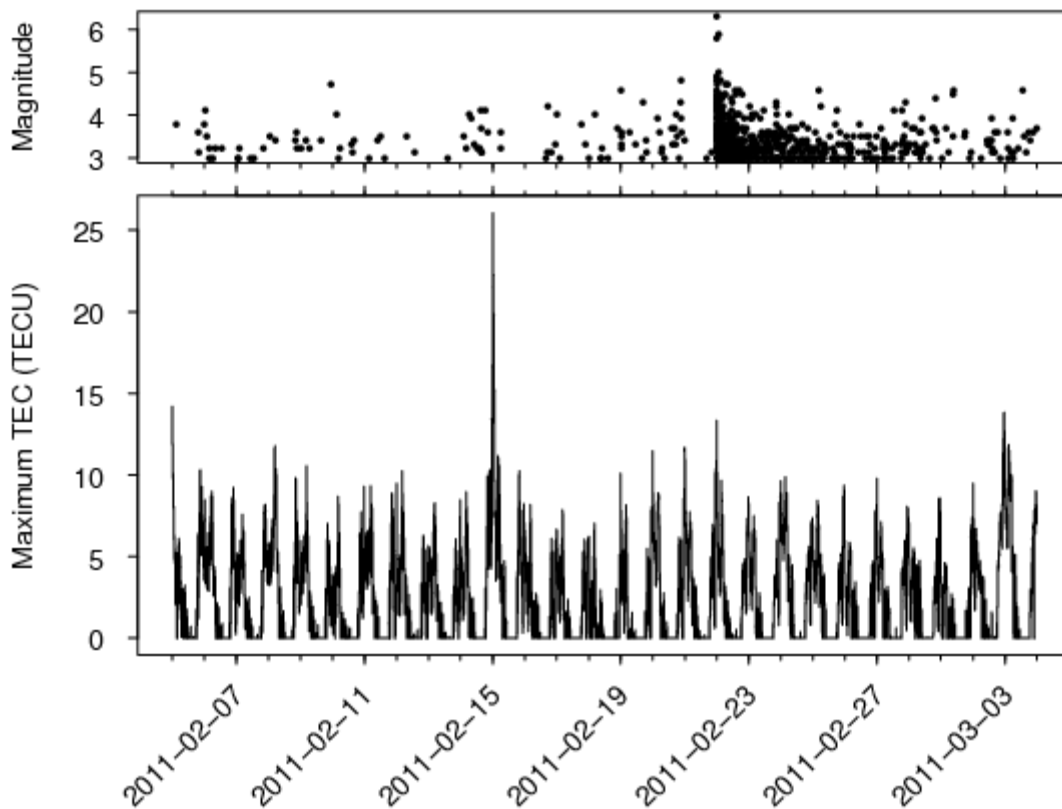


Figure 3 Lower: Maximum of TEC (y-axis) over the New Zealand region versus time in the period 2011/02/05 to 2011/03/03. Upper: Magnitude versus time of occurrence for earthquakes in the New Zealand region with magnitude $M \geq 3.0$, including the Christchurch earthquake of 2011/02/21.

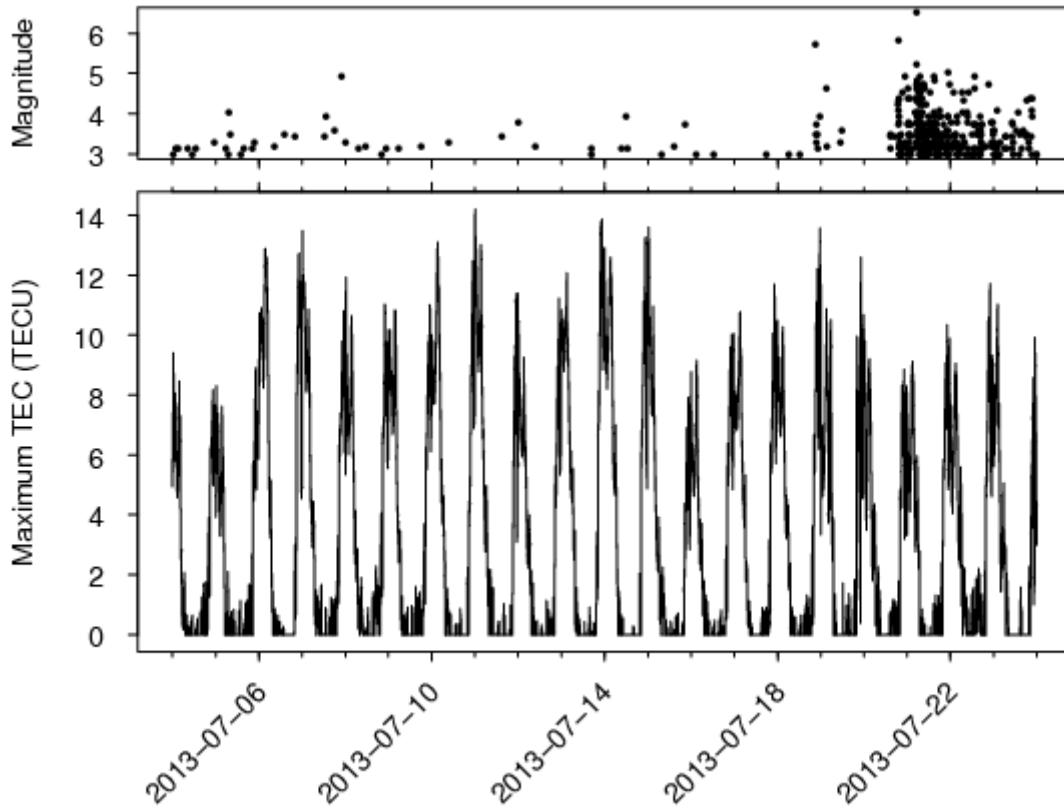


Figure 4 Lower: Maximum of TEC (y-axis) over the New Zealand region versus time in the period 2013/07/04 to 2013/07/23. Upper: Magnitude versus time of occurrence for earthquakes in the New Zealand region with magnitude $M \geq 3.0$, including the Seddon earthquake of 2013/07/21.

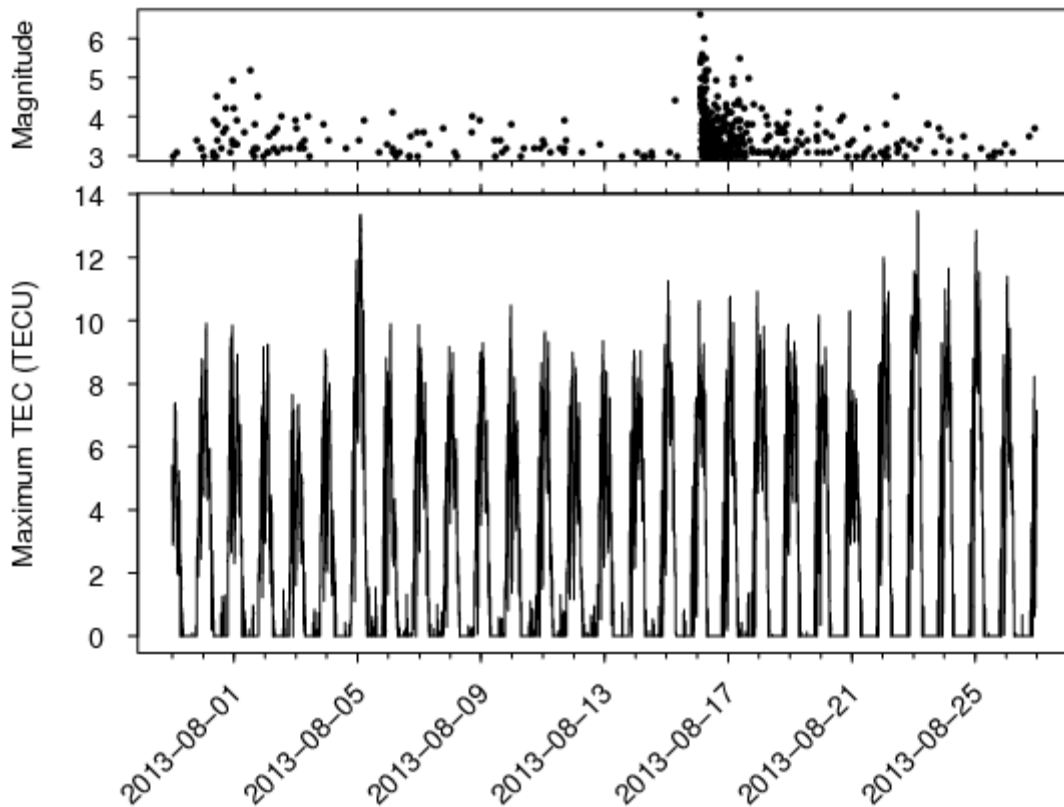


Figure 5 Lower: Maximum of TEC (y-axis) over the New Zealand region versus time in the period 2013/07/30 to 2013/08/26. Upper: Magnitude versus time of occurrence for earthquakes in the New Zealand region with magnitude $M \geq 3.0$, including the Lake Grassmere earthquake of 2013/08/16.

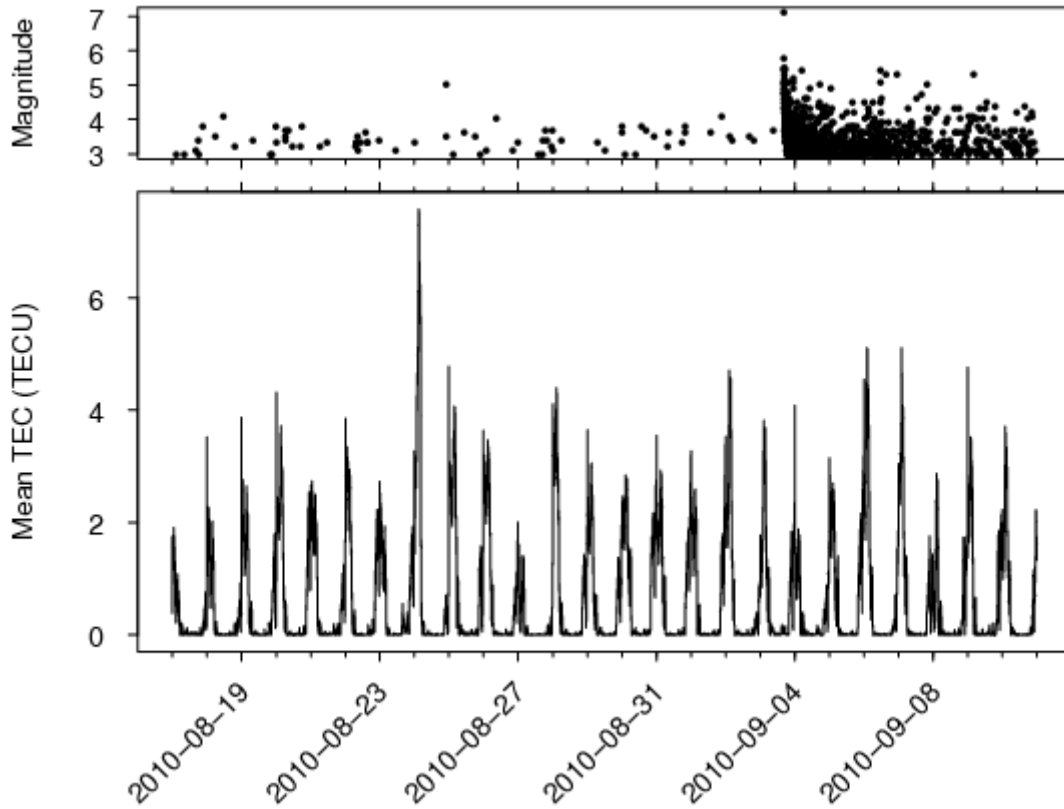


Figure 6 Lower: Mean of TEC (y-axis) over the New Zealand region versus time in the period 2010/08/17 to 2010/09/10. Upper: Magnitude versus time of occurrence for earthquakes in the New Zealand region with magnitude $M \geq 3.0$, including the Darfield earthquake of 2010/09/03.

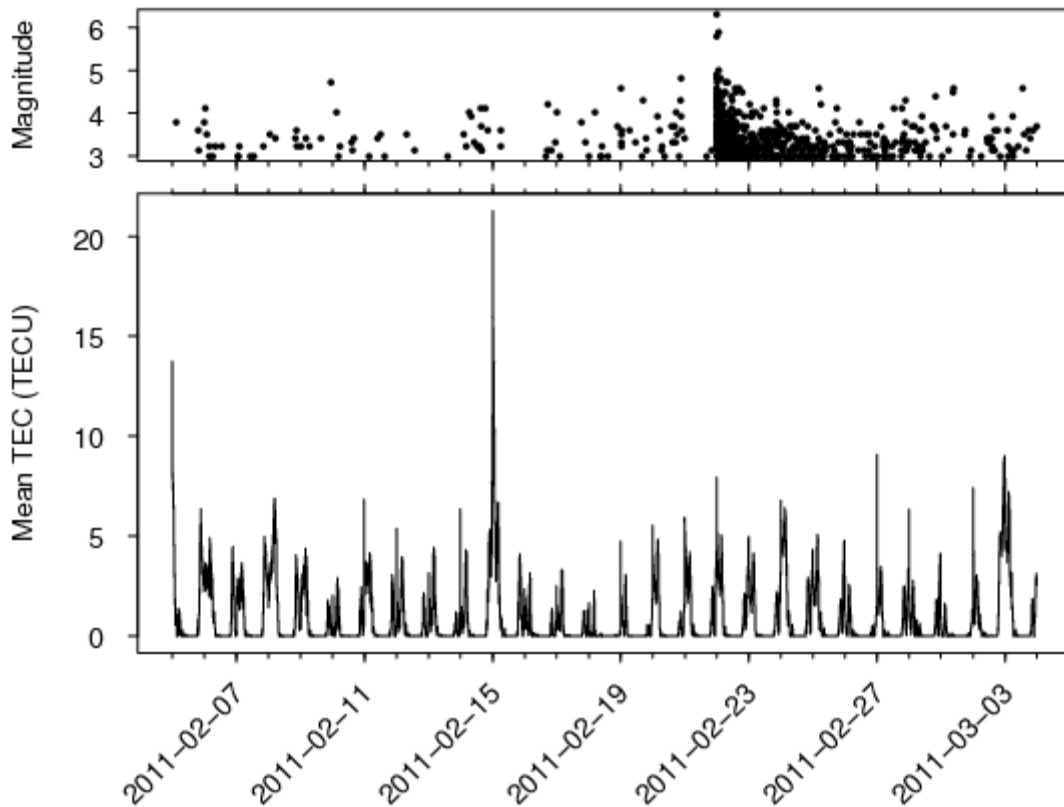


Figure 7 Lower: Mean of TEC (y-axis) over the New Zealand region versus time in the period 2011/02/05 to 2011/03/03. Upper: Magnitude versus time of occurrence for earthquakes in the New Zealand region with magnitude $M \geq 3.0$ versus time, including the Christchurch earthquake of 2011/02/21.

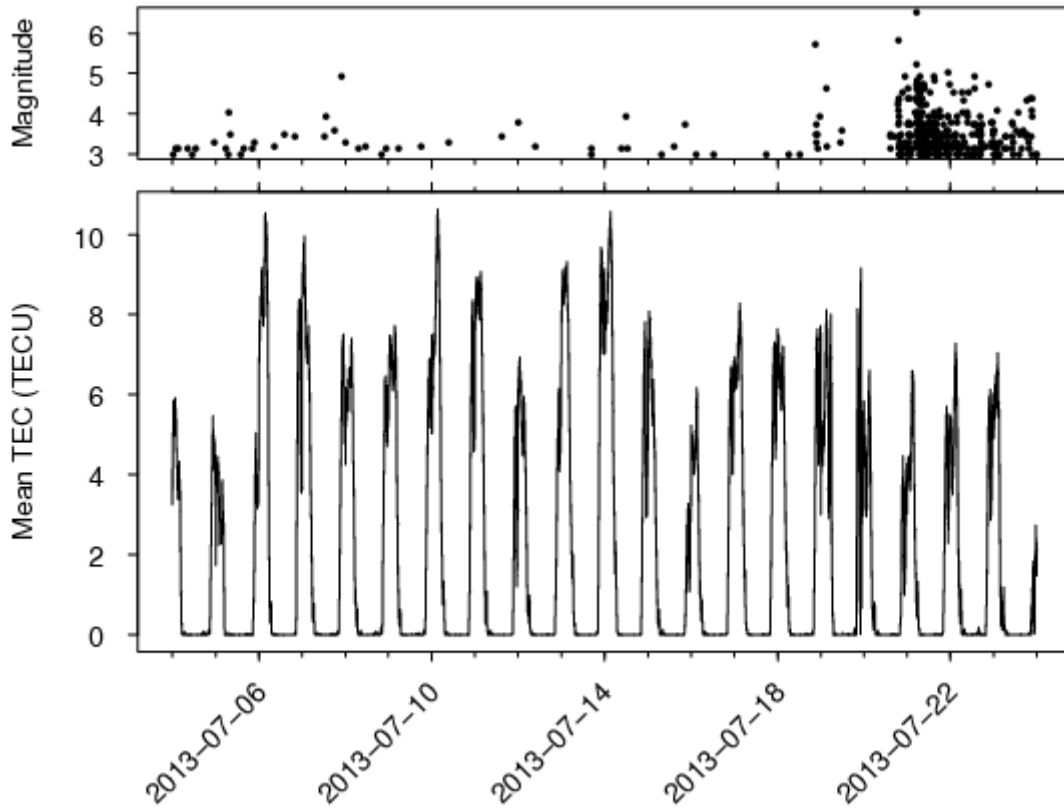


Figure 8 Lower: Mean of TEC (y-axis) over the New Zealand region versus time in the period 2013/07/04 to 2013/07/23. Upper: Magnitude versus time of occurrence for earthquakes in the New Zealand region with magnitude $M \geq 3.0$ versus time, including the Seddon earthquake of 2013/07/21.

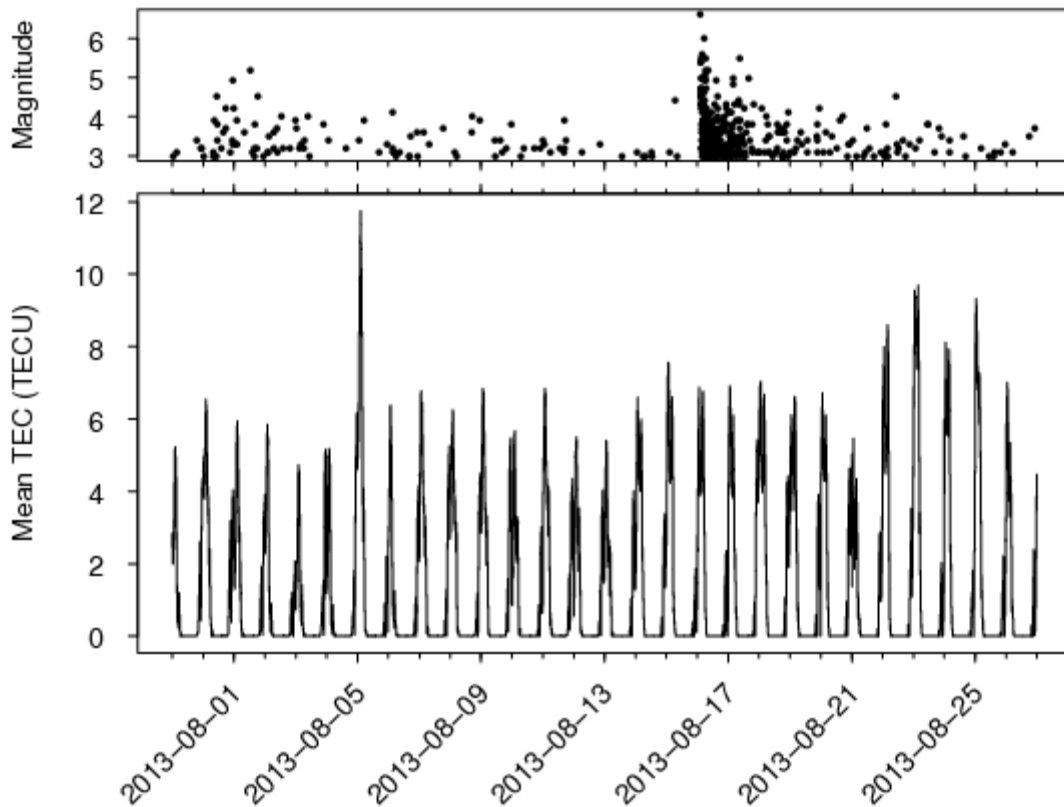


Figure 9 Lower: Maximum of TEC (y-axis) over the New Zealand region versus time in the period 2013/07/30 to 2013/08/26. Upper: Magnitude versus time of occurrence for earthquakes in the New Zealand region with magnitude $M \geq 3.0$ versus time, including the Lake Grassmere earthquake of 2013/08/16.

3.3 DEGREE OF ANOMALY SCALE

It is desirable to have an objective scale on which to measure the degree of anomaly of an extreme observation. We propose the following.

For a time series, $\{x(i), i = 1, \dots, n\}$, let x_{\max} denote the maximum value and x_u and x_l the upper and lower quartiles, respectively. The degree of anomaly of x_{\max} relative to x is defined as:

$$A(x_{\max}, x) = \frac{(x_{\max} - x_u)}{(x_u - x_l)}. \quad (3.1)$$

In other words, the degree of anomaly of an extreme value is the difference between the extreme and the upper quartile divided by the interquartile range. This non-parametric definition of anomaly is analogous to the identification of outliers in box-plots (Tukey, 1977). An outlier in a box plot is often taken as a value which is more than 1.5 times the interquartile range above the upper quartile (or below the lower quartile). By this analogy, any extreme value with a degree of anomaly greater than 1.5 would be regarded as an outlier of the distribution and therefore anomalous.

The degree of anomaly of an extreme minimum value can be measured in an analogous way, with the obvious adjustment to equation (3.1). An example of an extreme minimum arises in Section 4.2.

The degree of anomaly is calculated for the time series of daily extremes in maximum and mean TEC for the observation period before each major earthquake. Table 2 shows the lead time between the highest value of TEC and the major earthquake and the degree of TEC anomaly by this measure.

Table 2 Lead time and degree of anomaly of highest value of maximum and mean TEC in the lead up to each major earthquake.

Earthquake	Lead time (days)	Degree of anomaly (Maximum TEC)	Degree of anomaly (Mean TEC)
Darfield	11	1.63	2.24
Christchurch	7	4.10	3.75
Seddon	11	0.23	0.33
Lake Grassmere	11	0.99	4.19

According to the discussion above, the values in Table 2 indicate that the highest daily maxima of maximum and mean TEC prior to the Darfield and Christchurch earthquakes are anomalous by this measure. The highest daily maximum of mean TEC (but not maximum TEC) prior to the Lake Grassmere earthquake is also anomalous. However, there is no anomalously high daily maximum of TEC prior to the Seddon earthquake.

3.4 SPATIAL DISTRIBUTION OF TEC ANOMALIES

We examine the spatial distribution of TEC at the times of the anomalies prior to the Darfield, Christchurch and Lake Grassmere earthquakes.

Figure 10 and Figure 11 show the spatial distribution of TEC over the New Zealand region at the times of the anomalous maximum and mean TEC, respectively, preceding the Darfield earthquake. Figure 12 shows the spatial distribution of TEC at the time of the anomalous maximum and mean TEC preceding the Christchurch earthquake. Figure 13 shows the spatial distribution of TEC at the time of the anomalous mean TEC preceding the Lake Grassmere earthquake. The times of these anomalies (U.T.) are indicated in the header of the plots.

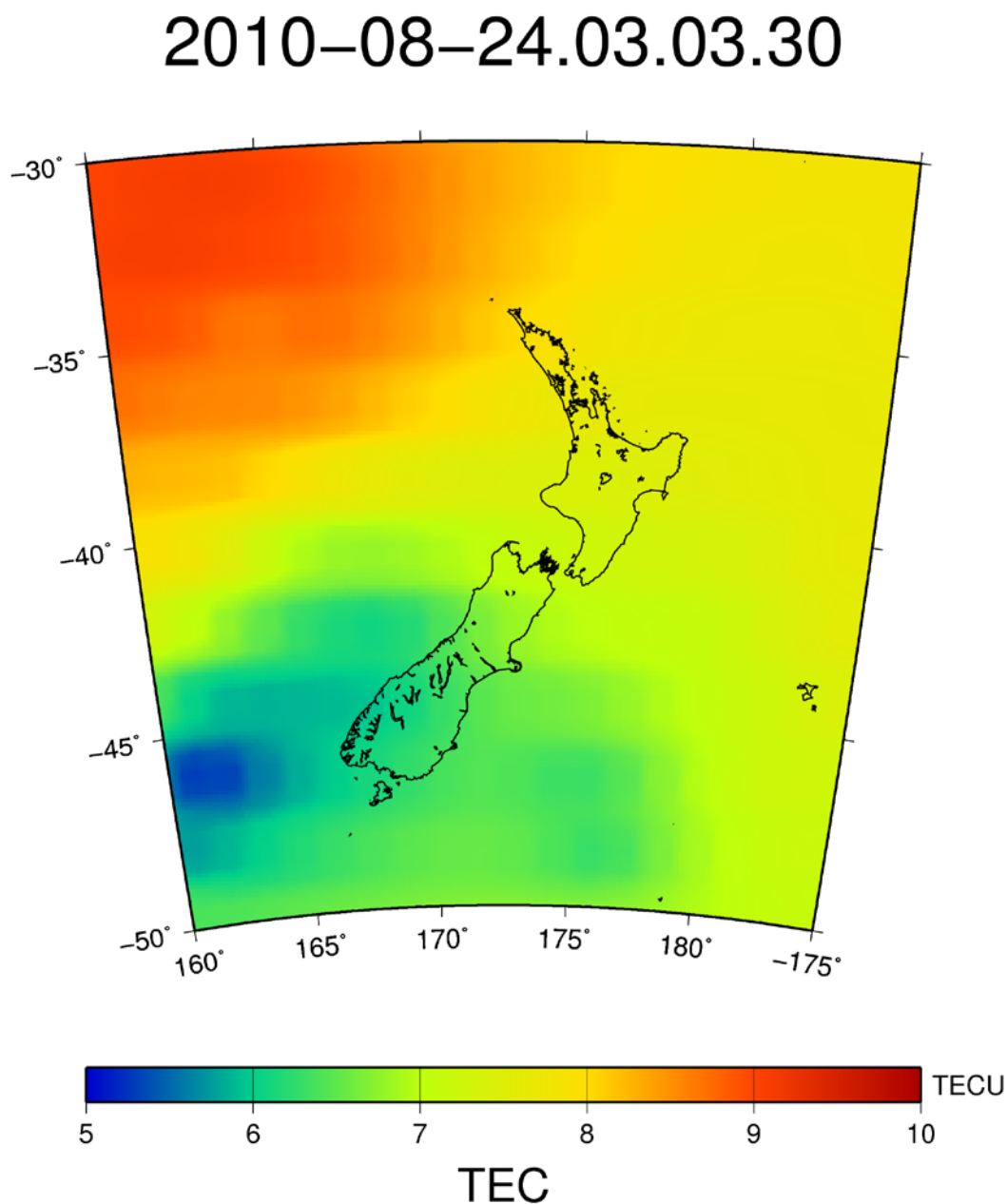


Figure 10 Spatial distribution of TEC over the New Zealand region at the time of the highest anomaly of maximum TEC preceding the Darfield earthquake.

In all cases the observed TEC distribution is not concentrated in the locality of the earthquake. In fact, in all cases the highest values of TEC are far offshore in the north east or north west of the mapped area. The lack of spatial correlation with the locations of earthquakes downgrades the credibility of the observed anomalies as earthquake precursors. More importantly, from the point-of-view of practical forecasting, it limits the information value of TEC anomalies as predictors of earthquakes, since the anomalies appear to contain no spatial information on the location of future earthquakes. Nevertheless, an anomaly occurring with a lead time of one to two weeks before a high proportion of large earthquakes, and rarely at other times, could still provide useful information gains.

2010-08-24.01.03.30

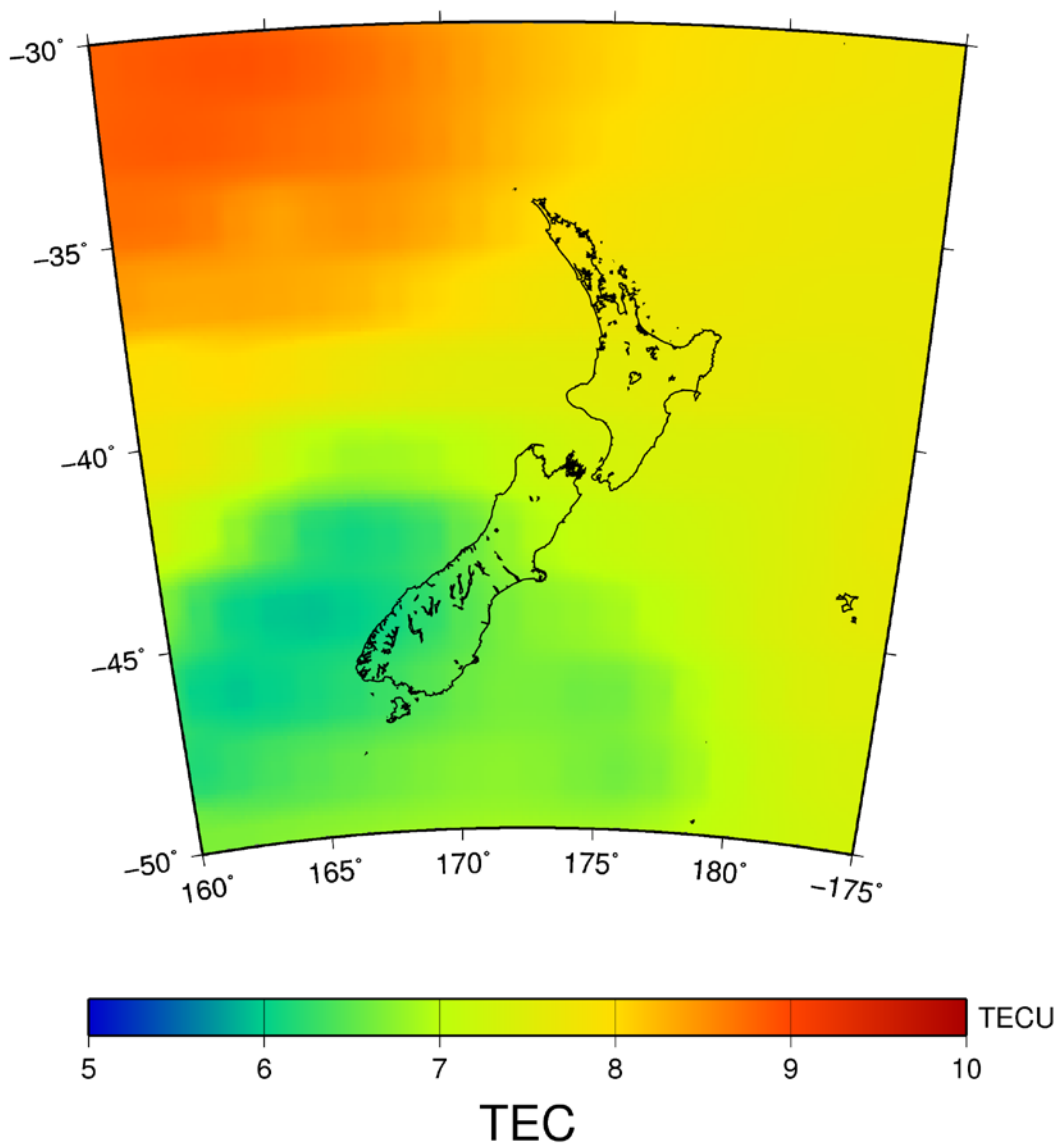


Figure 11 Spatial distribution of TEC over the New Zealand region at the time of the highest anomaly of mean TEC preceding the Darfield earthquake.

This analysis does not provide any information on the occurrence of TEC anomalies at other times. Therefore, based on this analysis, the usefulness of TEC anomalies as precursors of large earthquakes cannot be ruled out. However, there is at first glance nothing in the time-of-day of the observed anomalies (noon to early afternoon local time), or in the spatial distribution of TEC at the time of the anomalies, to suggest that the anomalies are related to physical processes in the Earth's crust close to the location of the subsequent major earthquakes. To the contrary, the anomalies appear to be most likely of solar or geomagnetic origin.

2011-02-15.00.00.30

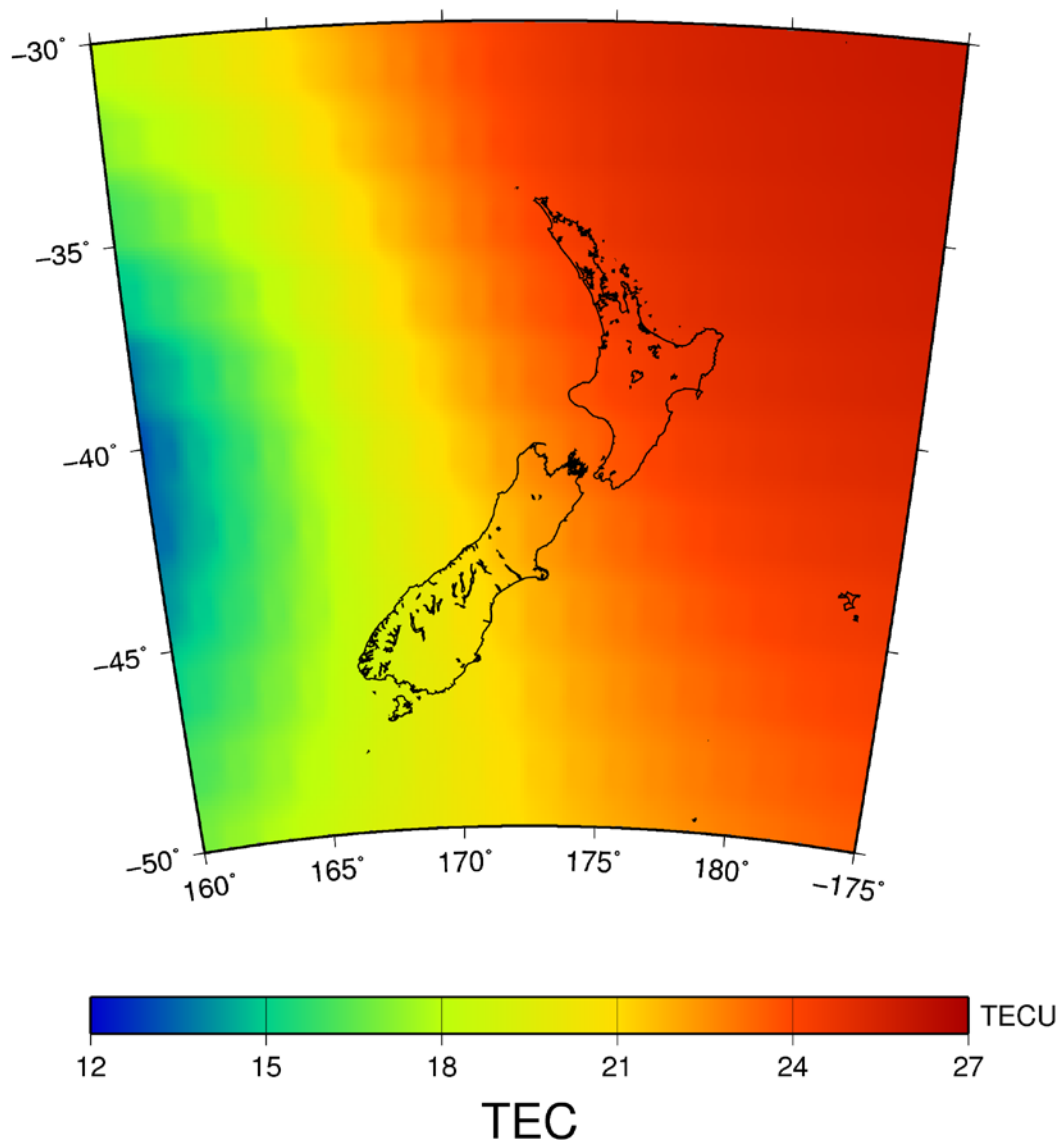


Figure 12 Spatial distribution of TEC over the New Zealand region at the time of the highest anomaly of maximum and mean TEC preceding the Christchurch earthquake.

3.5 COMPARISON WITH ANOMALIES OBSERVED IN PREVIOUS STUDIES

It is unlikely that the anomalies identified here are related to earthquake occurrence. These anomalies are different from examples of TEC anomalies in the literature. In terms of precursor time – the time between the observed anomaly and the subsequent major earthquake – the times in the present study (7–11 days) are somewhat longer than those typically reported in the literature, where the phrase “several days” is often used, or more specifically “1–7 days” (Pulinets, Gaivoranska et al., 2004).

2013-08-05.02.24.00

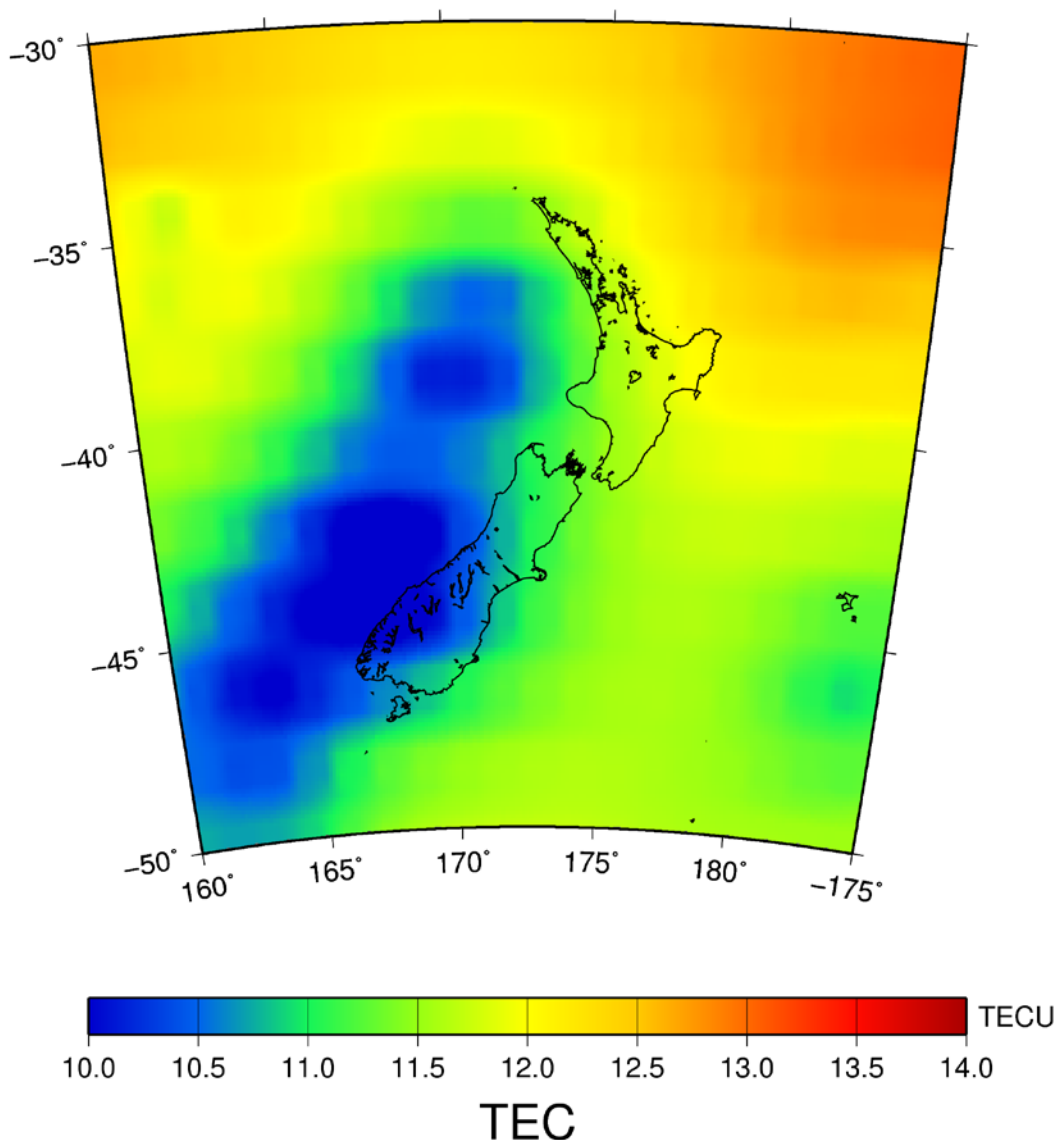


Figure 13 Spatial distribution of TEC over the New Zealand region at the time of the highest anomaly of mean TEC preceding the Lake Grassmere earthquake.

The anomalies recognised here are simple first-order effects, whereas in the literature a detailed cross-correlation analysis of TEC values close to the earthquake location and those farther away is used in order to reveal the anomalies. The type of anomaly typically observed is an increase in the variability of the TEC signal close to the earthquake source compared to the signals observed further away from the earthquake source; in other words, a breakdown in the correlation between TEC signals situated inside and outside of the seismogenic zone. Often these signals have to be extracted against a background of strong large scale temporal and spatial variations of TEC.

Our analysis so far has not looked for signals of the type usually observed as precursory anomalies, but only for large scale temporal and spatial variations of TEC. The earthquake-related signals, if they exist, are to be found only by a much more careful analysis of the temporal and spatial variability of TEC. The stronger the daily fluctuations in TEC are due to causes of solar origin, the more subtle the earthquake-related variations will appear to be, and the more sophisticated will be the analysis needed to extract them.

4.0 INDEX OF LOCAL TEC ANOMALY

We wish to define a gridded variable (index) which could become an input to hybrid earthquake likelihood forecasting models. Such a gridded variable would ideally be updated once per day – the shortest time period currently used for updating earthquake forecasts in the CSEP testing centres. In this section we propose an index which is a candidate to be used for this purpose. However, it is beyond the resources of this study, and would require a larger TEC data set than has been derived so far, to assess its worth for forecasting earthquakes.

Earthquake related variations of TEC are assumed to occur on a spatial scale comparable to the source region of a forthcoming earthquake. Normal fluctuations of TEC resulting from solar or geomagnetic influences generally occur on a larger spatial scale. The index should therefore be defined to distinguish smaller scale fluctuations of TEC from larger scale fluctuations.

Pulinets et al. (2004) described a correlation technique for revealing ionospheric precursors of earthquakes. It involves cross-correlating the intra-diurnal variations of TEC at two ground stations – an “internal” station within the earthquake preparation area and an “external” station outside the earthquake preparation area. The choice of the external ground station has to be such that it is close to the internal station in geomagnetic latitude (latitude measured in comparison the Earth’s magnetic poles), so that both stations would have similar reactions to geomagnetic disturbances. Also the longitude of the two stations should not differ too much because of the local time dependence of ionospheric reaction to geomagnetic storm commencement. The terms “close to” and “too much” were not quantified by Pulinets et al. (2004).

We adopt a similar approach here, but our locations of interest are not ground stations, but rather points in a grid of TEC estimates in the ionosphere. We wish to define a correlation index for each point in the grid. The index will have a daily value at each point of the grid and will describe the correlation of TEC during the day at each point compared with that at neighbouring points.

4.1 DEFINITION OF INDEX

Let $\{x(i, j, k), i = 1, \dots, I, j = 1, \dots, J; k = 1, \dots, K\}$ denote the space-time TEC observations at a grid of K locations over I days, at J evenly spaced times within each day. Suppose that grid-points within a distance D of grid-point k are close enough to have similar reactions to geomagnetic disturbances and similar ionospheric reaction to geomagnetic storm commencement. The set of grid points within distance D of k , but not including k itself, is denoted $N_D(k)$ and the number of grid points in this set is denoted $n_D(k)$. We define the local correlation index by:

$$C(i, k) = \frac{\sum_{j=1}^J (x(i, j, k) - \bar{x}(i, k))(y(i, j, k) - \bar{y}(i, k))}{(J-1)\sigma_x(i, k)\sigma_y(i, k)}, \quad (4.1)$$

where the daily mean of TEC at the k th grid location is

$$\bar{x}(i, k) = \sum_{j=1}^J \frac{x(i, j, k)}{J}, \quad (4.2)$$

the time-of-day mean of TEC in the neighbourhood of the k th grid location is

$$y(i, j, k) = \sum_{l \in N_D(k)} \frac{x(i, j, l)}{n_D(k)}, \quad (4.3)$$

the daily mean of TEC in the neighbourhood of the k th grid location is

$$\bar{y}(i, k) = \sum_{j=1}^J \frac{y(i, j, k)}{J}, \quad (4.4)$$

the daily variance of TEC at the k th grid location is

$$\sigma_x(i, k)^2 = \sum_{j=1}^J \frac{[x(i, j, k) - \bar{x}(i, k)]^2}{J - 1}, \quad (4.5)$$

and the daily variance of TEC in the neighbourhood of the k th grid location is

$$\sigma_y(i, k)^2 = \sum_{j=1}^J \frac{[y(i, j, k) - \bar{y}(i, k)]^2}{J - 1}. \quad (4.6)$$

By definition, the correlation index takes values in the interval $[-1, 1]$. We expect that the index will nearly always be greater than zero, and that most values will be close 1, because of the correlation induced by large scale solar and geomagnetic influences.

If the correlation index is very close to 1 for a given point in the spatial grid, there is no deviation of the temporal pattern of TEC variation at the grid point from that in the wider area surrounding it. In that case, it may be concluded that there are no local disturbances to the large scale pattern of TEC created by solar and geomagnetic effects. If the correlation index is appreciably less than 1, then there is evidence of a local disturbance to the TEC field variation, and earthquake induced effects are a possible cause of this anomaly.

The correlation index, and indeed the TEC maps themselves, obviously depend to some extent on the density of the GPS station network, the density of the satellite array, and the grid density (Figure 1). These dependencies are not investigated here. However, it is notable that the present network of continuous GPS stations in New Zealand is considerably denser in the North Island than the South Island, and that the grid density in Figure 1 is sparse in comparison to the GPS station densities even in the South Island. In some cases the nearest grid point to an earthquake source may be tens of kilometres away. It is not known what impact this may have on the ability of the index to detect precursory TEC anomalies, if they exist.

4.2 PLOTS OF LOCAL CORRELATION INDEX

Using a distance threshold of $D = 250$ km, we computed the local correlation index $C(i, k)$ for the grid location nearest to the epicentre of each of the four major earthquakes (Table 1). For this value of D , we have $n_D(k) = 10$ for most grid locations, except for those on the edge of the grid (see Figure 1). For each major earthquake, we plotted the index as a function of time for the grid point nearest to earthquake epicentre (Figure 14).

For the Darfield, Seddon and Lake Grassmere events there was no appreciable change in the local correlation during the pre-earthquake and post-earthquake period. The correlation remained close to one throughout the period plotted. For the Christchurch earthquake there was a dip in the correlation starting 5 days before the earthquake. The correlation reached a minimum value of 0.84 on 18 February 2011, three days before the Christchurch earthquake, and recovered to a value close to one before the earthquake. There was a smaller dip in the correlation five days after the earthquake.

The dip in the correlation before the Christchurch earthquake is similar to the proposed ionospheric earthquake precursors reported in the literature. The timing of the dip fits well within the range of one to seven days before the earthquake as reported by Pulinets et al. (2004). The size of the dip is also within the range of examples of cross correlation of the ionospheric F (upper) layer critical frequency foF2 between two stations – one inside the earthquake preparation area and one outside. The critical frequency is the limiting frequency below which a wave component is reflected by, and above which it penetrates through, an ionospheric layer.

The background level of the correlation here is much more stable and consistently close to one in this study than in the Pulinets et al. (2004). A difference between the two studies is that here we are correlating 2880 observations at 30 second intervals within each daily period, whereas Pulinets et al (2004) correlated only 24 hourly readings per day. Also, it is possible that the interpolation and smoothing procedures that the GPSTk software uses to compute the spatial grid of TEC values may increase the spatial correlations in the present study.

2011-02-18

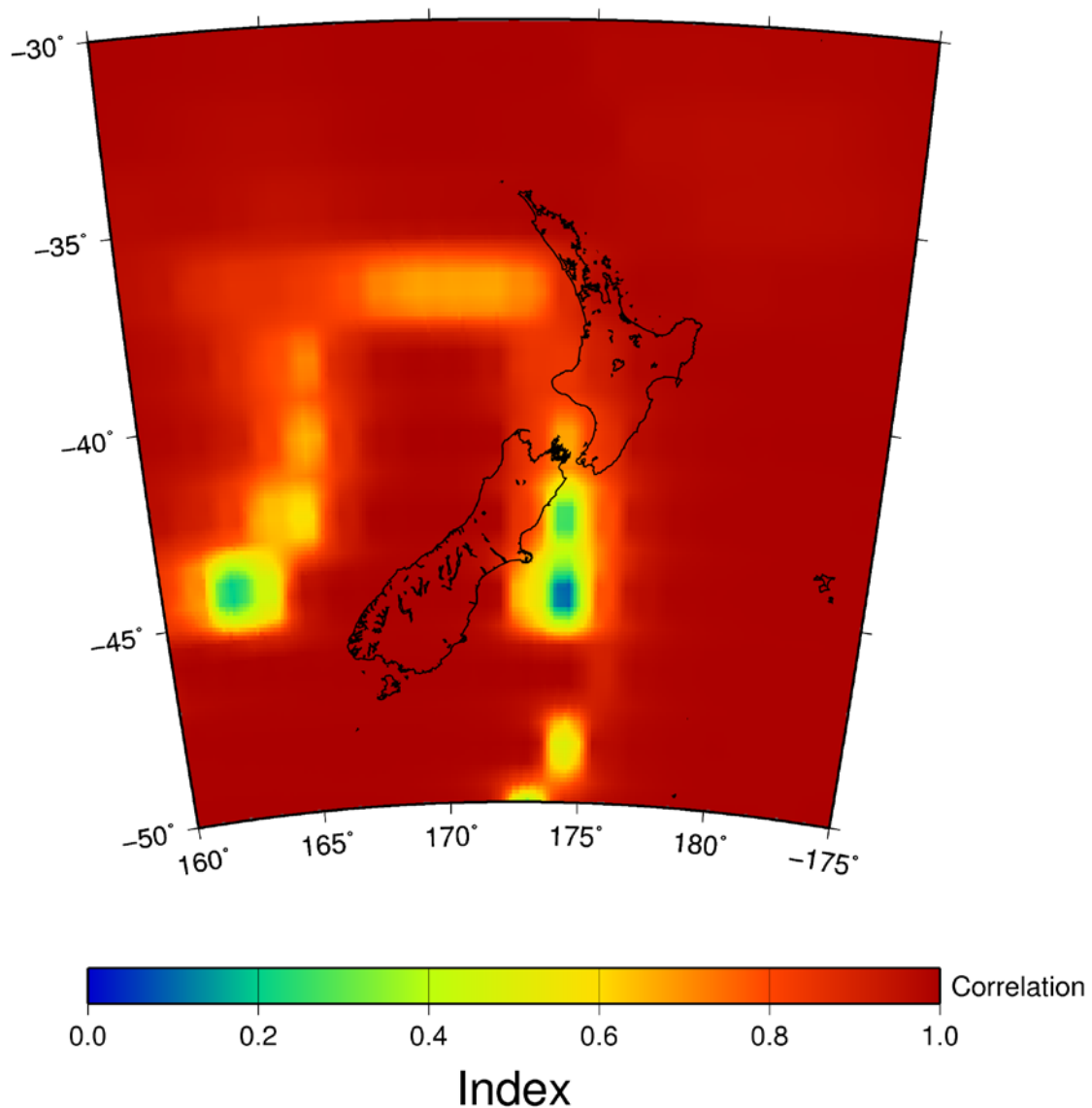


Figure 15 Spatial variation of local correlation index on 18 February 2011, the time of greatest anomaly in the index prior to the Christchurch earthquake.

The low value of the correlation index on 18 February 2011 constitutes an anomaly in the time series, as defined in Section 3.3, with a degree of anomaly of 26.7 (c.f. the maximum degree of anomaly of 4.19 in Table 2). However there are other similarly low and lower correlations at other grid points on the same day. Figure 15 shows the spatial distribution of the local correlation index on 18 February 2011. The lowest correlations are located in a patch covering about five degrees of latitude and four degrees of longitude to the east of the South Island. The western edge of this patch, which has two centres – about 150 km north-east and south-east of Christchurch – includes Christchurch itself. Another anomalously low patch is located about 600 km from Christchurch off the west coast of the South Island. Both of these patches are part of a wider region of low correlations bordering, on three sides, a high-correlation area of about 13 degrees in latitude and five degrees of longitude. We have no explanation for the spatial distribution of the anomaly.

Of all the days for the correlation index was calculated, 18 February shows the largest area of low correlation and the lowest values of the local correlation index.

During the whole time period considered in relation to the Seddon and Lake Grassmere earthquakes – from 4 July 2013 to 26 August 2013 – no value of the local correlation index lower than 0.99 was observed for any location.

It is impossible to establish the source of any given anomaly. The localness of the anomaly on 18 February 2011 suggests that it is not of solar or geomagnetic origin. The precursor time of three days and the concentration of spatial anomalies at locations not far from Christchurch suggest that the anomaly could be associated with the preparation process of the Christchurch earthquake. However, Kane (2011) reported a strong solar flare on 15 February 2011, followed by a coronal mass ejection which caused a weak geomagnetic anomaly on 18 February 2011, coinciding approximately with the time of the TEC anomaly near Christchurch. It is possible that the TEC anomaly is a local effect of the geomagnetic anomaly. However, we note that the TEC anomaly began on 16 February and ended on 19 February, whereas the geomagnetic anomaly reported by Kane (2011) began early on 18 February and lasted less than 24 hours.

Perhaps further detailed analyses of the temporal and spatial geomagnetic and TEC variation during the time between the solar flare and the time of the Christchurch earthquake would provide further evidence as to whether or not the TEC anomaly is related to earthquake occurrence. However, such an analysis would probably be time consuming and the outcome, whatever it might be, would only be of anecdotal value. The over-riding goal of the present study is to move the study of ionospheric earthquake precursors from the anecdotal to the testing stage. Therefore, it is less important to analyse particular examples of precursory anomalies in detail than it is to establish the overall information gain of all observed anomalies in earthquake forecasting. The latter objective is best achieved by extending the present database of TEC anomalies and using it as an input for fitting hybrid earthquake forecasting models.

5.0 CONCLUSION

The present pilot study has achieved most of its objectives, although the data set of TEC observations covers a shorter time period overall than was expected at the outset. The adaptation of the GPSTk software for computation of ionospheric TEC from GPS observations over New Zealand has been accomplished and has been shown to work well. Extension of the TEC data set to a much longer period requires accessing sufficient high performance computing resources and automating running of the software. This is a problem that will be overcome either as high performance computing resources now available are exploited or more resources become available to us in the future.

The local correlation index defined here has been shown to be capable of detecting local anomalies in TEC similar to those reported in the literature. It is clear that this type of TEC anomaly does not occur consistently before medium-to-large earthquakes, because a short-term precursory TEC anomaly is seen for only one of the four earthquakes studied. Also, anomalies are occasionally seen at other times and locations apparently unrelated to earthquake occurrence. Therefore, like all other precursors identified to date, TEC anomalies are unlikely to be a “silver bullet” for earthquake prediction in the sense of Jordan (2006). Nevertheless, if even a minor proportion of major earthquakes have short-term ionospheric precursors, the information gain from including them in an earthquake forecasting system could be considerable.

It is proposed therefore to continue this line of research in the direction originally contemplated, subject to available resources and integrated with other efforts to improve earthquake forecasting. This will involve extending the present database of atmospheric TEC to a longer time period, and computing and storing the grid of local correlation index for each day. These daily grids are potential inputs to hybrid earthquake forecasts, along with the earthquake catalogue and other data possibly related to earthquake occurrence. The value of TEC as an earthquake precursor will then be measured by the information gain when it is incorporated in a hybrid earthquake forecasting model (Rhoades et al., 2014) which already includes the best model derived from all other inputs.

The distance parameter D in the local correlation index was arbitrarily chosen to be 250 km in this study. An investigation of the best value to use could be undertaken when a larger set of precursory anomalies is available.

6.0 ACKNOWLEDGEMENTS

This study was supported by the Earthquake Commission Research Foundation under grant number BIE 10/591. The report has been internally reviewed by Annemarie Christophersen and Sigrun Hreinsdottir.

7.0 REFERENCES

- Afraimovich, E.L. and Astafaya, E.I. 2008. TEC anomalies-Local TEC changes prior to earthquakes or TEC response to solar and geomagnetic activity changes? *Earth Planets Space*, 60(9): 961–966.
- Calais, E. and Minster, J.B. 1995. GPS detection of ionospheric perturbations following the January 17, 1994, Northridge earthquake, *Geophys. Res. Lett.*, 22: 1045–1048.
- Chen, Y.I., Liu, J.Y., Tsai, Y.B. and Chen, C.S. 2004. Statistical tests for pre-earthquake ionospheric anomaly, *Terr. Atm. Ocean Sci.*, 15: 385–396.
- Dautermann T., Calais E., Haase J. and Garrison J. 2007. Investigation of ionospheric electron content variations before earthquakes in southern California, 2003–2004. *Journal of Geophysical Research*, 112(B2): B02106, doi:10.1029/2006JB004447.
- Gaussiran, T.L., Munton, T.D., Harris, B. and Tolman, B. 2004. An Open Source Toolkit for GPS Processing, Total Electron Content Effects, Measurements and Modeling International Beacon Satellite Symposium 2004 Trieste, Italy October, 2004.
- Hayakawa, M. 2007. VLF/LF Radio Sounding of Ionospheric Perturbations Associated with Earthquakes, *Sensors* 7: 1141–1158.
- Jordan, T.H. 2006. Earthquake predictability, brick by brick. *Seismological Research Letters*, 77(1): 3–6.
- Kane, R.P. 2011. Solar flare of 15 February 2011 and its geomagnetic effects, *Indian Journal of Radio & Space Physics*, 40: 253–256.
- Kim, V.P. and Hegai, V.V. 1997. On possible changes in the mid-latitude upper ionosphere before strong earthquakes, *J. Earthq. Predict. Res.*, 6: 275–280.
- Liu, J.Y., Chen, Y.I., Pulnits, S.A., Tsai, Y.B. and Chuo, Y.J. 2000. Seismo-ionospheric signatures prior to M = 6.0 Taiwan earthquakes, *Geophysical Research Letters*, 27: 3113–3116.
- Liu, J.Y., Chen, Y.I., Chuo, Y.J. and H.F. Tsai 2001. Variations of ionospheric total content during the Chi-Chi earthquake. *Geophys. Res. Lett.*, 28: 1381–1386.
- Liu, J.Y., Chuo, Y.J., Pulnits, S.A., Tsai, H.F. and Zeng, X. 2002. A study on the TEC perturbations prior to the Rei-Li, Chi-Chi and Chia-Yi earthquakes. In: Hayakawa M. and O. A. Molchanov (Eds.), *Seismo-Electromagnetics: Lithosphere-Atmosphere-Ionosphere Coupling*, TERRAPUB, Tokyo, 297-301p.
- Liu, J.Y., Chuo, Y.J., Shan, S.J., Tsai, Y.B., Pulnits, S.A. and Yu, S.B. 2004. Pre-earthquake ionospheric anomalies monitored by GPS TEC. *Ann. Geophys.*, 22: 1585–1593.
- Manucci, A., Wilson, B. and Edwards, C. 1993. A new method for monitoring the Earth's ionospheric total electron content using the GPS global network, in *ION GPS-93*, pp. 22– 24, Inst. of Navig., Fairfax, Va.

- Pulinets, S.A. 2004. Ionospheric precursors of earthquakes; recent advances in theory and practical applications. *TAO*, 15(3), 413–435.
- Pulinets, S. 2007. Natural radioactivity, earthquakes, and the ionosphere. *EOS*, 88: 217–218.
- Pulinets, S.A. and Boyarchuk, K.A. 2004. *Ionospheric Precursors of Earthquakes*, Springer Verlag, Berlin, Germany, 315pp.
- Pulinets, S.A., Boyarchuk, K.A., Hegai, V.V., Kim, V.P. and Lomonosov, A.M. 2000. Quasielectrostatic model of atmosphere-thermosphere-ionosphere coupling. *Advances in Space Research*, 26: 1209–1218.
- Pulinets, S.A., Gaivoronska, T.B. and Ciralo, L. 2004. Correlation analysis technique revealing ionospheric precursors of earthquakes, *Natural Hazards and Earth Science Systems*, 4: 697–702.
- Pulinets, S.A., Legen'ka, A.D., Gaivoronskaya, T.V. and Depuev, V.Kh. 2003. Main phenomenological features of ionospheric precursors of strong earthquakes, *J. Atmos. Solar-Terr. Phys.*, 65: 1337–1347.
- Pulinets, S.A. and Legen'ka, A.D. 2003. Spatial-temporal characteristics of the large scale disturbances of electron concentration observed in the F-region of the ionosphere before strong earthquakes, *Cosm. Res.*, 41: 221–229.
- Pulinets, S.A. and Liu, J.Y. 2004. Ionospheric variability unrelated to solar and geomagnetic activity, *Advances in Space Research*, 34: 1926–1933.
- Rhoades, D.A., Gerstenberger, M.C., Christophersen, A., Zechar, J.D., Schorlemmer, D., Werner, M. and Jordan, T.H. 2014. Regional earthquake likelihood models: Information gains of multiplicative hybrids. *Bulletin of the Seismological Society of America*, 104(6): 3072–3083.
- Saroso, S., Liu, J.Y., Hattori K. and Chen, C.H. 2008. Ionospheric GPS TEC Anomalies and $M \geq 5.9$ Earthquakes in Indonesia during 1993–2002, *Terrestrial Atmospheric and Oceanic Sciences*, 19(5): 481–488.
- Schorlemmer, D., Gerstenberger, M.C., Wiemer, S., Jackson, D.D. and Rhoades, D.A. 2007. Earthquake likelihood model testing. *Seismological Research Letters*, 78(1): 17–29.
- Sorokin, V.M., Chmyrev, V.M. and Hayakawa, M. 2000. The formation of ionosphere-magnetosphere ducts over the seismic zone. *Planet. Space Sci.*, 48: 175–180.
- Surotkin, V.A., Klimenko, V.V., and Koren'kov, Yu.N. 2007. Model calculations of the total electron count for the GPS satellites system, *International Journal of Geomagnetism and Aeronomy*, 7, GI1002, doi:10.1029/2005GI000106.
- Tukey, J.W. 1977. *Exploratory Data Analysis*. Addison-Wesley. ISBN 0-201-07616-0. OCLC 3058187
- Uyeda, S., Nagao, T. and Kamogawa, M. 2009. Short-term earthquake prediction: Current status of seismo-electromagnetics, *Tectonophysics*, 470: 205–213.
- Zakharenkova I.E., Shagimuratov I.I., and Krankowski, A. 2007. Features of the ionosphere behavior before the Kythira 2006 earthquake, *Acta Geophysica*, 55(4): 524–534.
- Zhou Y., Wu Y., Qiao X. and Zhang, X. 2009. Ionospheric anomalies detected by ground-based GPS before the Mw7.9 Wenchuan earthquake of May 12, 2008, *China Journal of Atmospheric and Solar-Terrestrial Physics*, 71(8–9): 959–966.



www.gns.cri.nz

Principal Location

1 Fairway Drive
Avalon
PO Box 30368
Lower Hutt
New Zealand
T +64-4-570 1444
F +64-4-570 4600

Other Locations

Dunedin Research Centre
764 Cumberland Street
Private Bag 1930
Dunedin
New Zealand
T +64-3-477 4050
F +64-3-477 5232

Wairakei Research Centre
114 Karetoto Road
Wairakei
Private Bag 2000, Taupo
New Zealand
T +64-7-374 8211
F +64-7-374 8199

National Isotope Centre
30 Gracefield Road
PO Box 31312
Lower Hutt
New Zealand
T +64-4-570 1444
F +64-4-570 4657